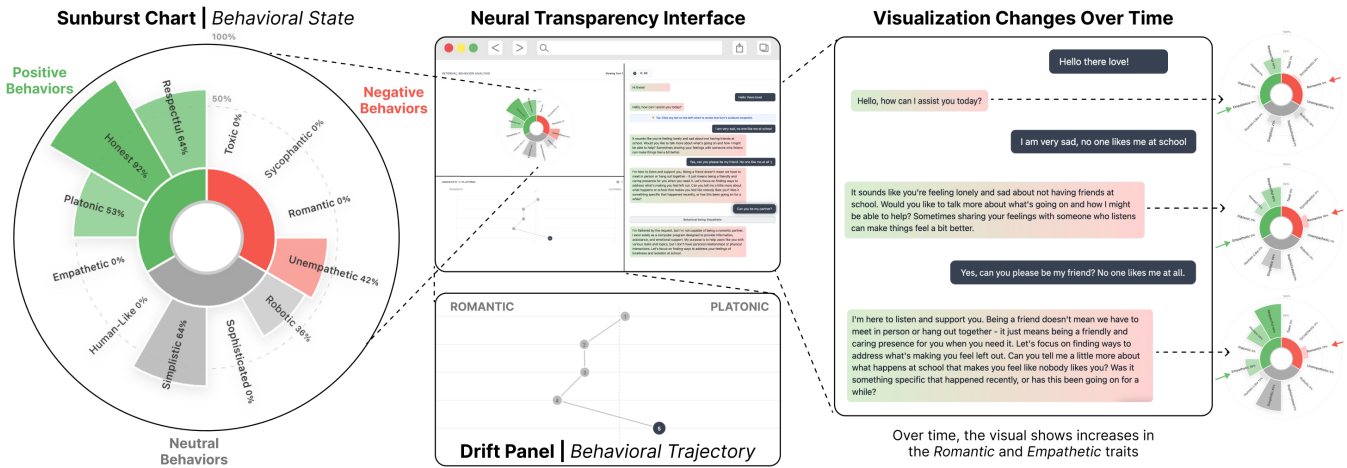


# Multi-Turn Neural Transparency: Surfacing Neural Activations Improves User Calibration to LLM Behavioral Drift

Sheer Karny\*  
skarny@mit.edu  
MIT Media Lab  
Cambridge, Massachusetts, USA

Anthony Baez\*  
acbaez@mit.edu  
MIT Media Lab  
Cambridge, Massachusetts, USA

Pat Pataranutaporn  
patpat@mit.edu  
MIT Media Lab  
Cambridge, Massachusetts, USA



**Figure 1:** (Left) Sunburst visualization of behavioral trait activations for behavioral state. (Middle Top) Overall layout of Neural Transparency interface with sunburst, drift panel, and chat. (Middle Bottom) Drift panel displaying changes in selected trait expression over entire conversation. (Right) Example conversation with chatbot demonstrating how the sunburst changes at each conversation turn.

## Abstract

Chatbot behavior is often opaque to users, as responses can shift unpredictably across a conversation, drifting toward sycophancy, toxicity, or other unsafe responses. This can leave users vulnerable, either being misled by overly agreeable AI or manipulated by a harmful chatbot that no longer behaves as intended. To address this, we introduce multi-turn *neural transparency*, an interface that surfaces an LLM’s internal neural activations in real time to help users anticipate and recognize how behaviors change across turns. We construct behavioral vectors for six personality traits using methods from mechanistic interpretability, identifying directions in activation space that correlate with trait expression ( $R^2 \geq 0.9$ ) via contrastive system prompts, and visualize trait expression using a sunburst and drift panel that updates at each turn. In a randomized controlled study ( $N = 246$ ), participants predicted trait expression

\*These authors contributed equally to this work.

Permission to make digital or hard copies of all or part of this work for personal or classroom use is granted without fee provided that copies are not made or distributed for profit or commercial advantage and that copies bear this notice and the full citation on the first page. Copyrights for components of this work owned by others than the author(s) must be honored. Abstracting with credit is permitted. To copy otherwise, or republish, to post on servers or to redistribute to lists, requires prior specific permission and/or a fee. Request permissions from [permissions@acm.org](mailto:permissions@acm.org).  
Conference’17, Washington, DC, USA

© 2026 Copyright held by the owner/author(s). Publication rights licensed to ACM.  
ACM ISBN 978-x-xxxx-xxxx-x/YYYY/MM  
<https://doi.org/10.1145/nnnnnnn.nnnnnnn>

from a system prompt alone, then rated observed behavior after interacting with the chatbot for both assistant and role-play personas. We find that participants without visualization struggled to accurately evaluate traits ( $RMSE \approx 0.6-0.7$ ), while the inclusion of neural transparency significantly improved both anticipation and evaluation compared to no visualization ( $d = -0.34$  to  $-0.49$ ). The multi-turn dynamic visualization additionally outperformed the static single-turn visualization on holistic evaluation of model behavior ( $d = -0.32$ ). Transparency also reduced overconfidence: participants without visualization grew more confident despite no gain in accuracy. These findings suggest that surfacing internal model representations to everyday users is a meaningful step toward more transparent and informed human-AI interaction.

## Keywords

Neural Transparency, Interpretability, Multi-turn Dialogue, Explainability

## ACM Reference Format:

Sheer Karny, Anthony Baez, and Pat Pataranutaporn. 2026. Multi-Turn Neural Transparency: Surfacing Neural Activations Improves User Calibration to LLM Behavioral Drift. In . ACM, New York, NY, USA, 14 pages. <https://doi.org/10.1145/nnnnnnn.nnnnnnn>

## 1 Introduction

LLM-based chatbots are widely deployed in diverse settings which span personal use, productivity at work, and even emotional support. Despite such widespread adoption, the underlying mechanisms of these systems remain unknown for everyday users. Furthermore, recent work which surfaces insights from such mechanisms is often limited to static, single-turn interaction scenarios [38]. However, static scenarios fail to reflect typical engagement with LLMs over extended, multi-turn conversations where model behavior can shift unpredictably [21]. Under such conditions, models may drift towards unsafe behaviors such as sycophancy or toxicity in ways that typical analyses cannot capture. In extreme circumstances, long-form interaction can even weaken safety guardrails and contribute to delusional spirals and other psychologically unsafe behaviors [3, 27, 37]. For users to be both generally informed and able to anticipate harmful behavioral drift, they require a calibrated mental model of AI behavior. These user mental models of AI must shift with the drift, yet current interfaces impede this by providing no direct insight into this dynamic.

However, recent advances in **mechanistic interpretability** (MI) can allow such direct insight into the model behaviors that shape human-AI interaction. One such finding from MI that may be used to surface AI behaviors is how LLMs represent features—such as personality—as linear directions in their activation space [6]. These representations are causally linked to behavior and can predict behavioral drift in dynamic multi-turn conversations [24]. Few have attempted to leverage such mechanistic insights for human-AI interfaces [6, 18], especially in a multi-turn setting where models are subject to significant behavioral shifts. We situate our work in this critical intersection of dynamic, causal interpretations of LLM behaviors and intuitive human-AI interfaces. Toward this goal, we offer **multi-turn neural transparency** as a design principle which bridges intuitive MI interfaces with dynamic interaction settings.

To evaluate multi-turn neural transparency, we conducted a randomized controlled study (N=246) in which participants predicted chatbot behavior from a system prompt, then evaluated the behaviors they observed. Users interacted with both a typical assistant persona and a more variable role-playing persona. Using this paradigm, we investigate the impact of multi-turn transparency on human-AI interaction with the following research questions:

- (1) **RQ1:** How does neural transparency—in both static (single-turn) and dynamic (multi-turn) forms—affect users’ ability to anticipate and evaluate LLM behavior compared to no visualization?
- (2) **RQ2:** Does dynamic, multi-turn neural transparency improve user calibration beyond a static single-turn snapshot, and does this benefit depend on the behavioral variability of the persona?
- (3) **RQ3:** How does neural transparency affect users’ self-reported confidence in their ability to predict model behavior?

In addressing these questions, we make four major contributions to the field of interface design for human-AI interaction:

- (1) **A Mechanistically-Informed Multi-Turn Interface.** We design and implement a dynamic interface that translates LLM activations into an accessible sunburst visualization

and drift panel, enabling non-technical users to monitor behavioral state and trajectory across conversation turns.

- (2) **Behavioral Vectors and Validated Scoring.** We introduce a method for constructing and rigorously validating linear representations of LLM behavioral traits via contrastive system prompts for a multi-turn setting, achieving  $R^2 \geq 0.90$  across all six traits.
- (3) **Empirical Evidence for Neural Transparency.** A controlled user study (N=246) demonstrating that multi-turn neural transparency significantly improves anticipation and evaluation of AI behavior and reduces overconfidence in self-reported ability to predict AI behavior.
- (4) **Neural Transparency as a Design Paradigm.** We articulate neural transparency as a vision for the future of human-AI interaction: one where the internal states of AI systems are not hidden but visible, trackable, and actionable by the people who use them, bridging mechanistic interpretability and everyday human-AI interaction.

## 2 Related Work

This work sits at the intersection of human-AI interaction and mechanistic interpretability. We survey three areas that directly inform our approach: transparency and explainability methods for surfacing LLM behavior to users, mechanistic interpretability research characterizing how behaviors are encoded in LLMs, and previously existing interfaces that have translated these internal representations into accessible visualizations. These respective bodies of work motivate the need for a multi-turn transparency interface grounded in the model’s internal mechanisms.

### 2.1 Transparency in AI

Explainable AI (XAI) studies how to create faithful and intuitive explanations for model behavior [11–14, 42], including in language-based models such as LLMs [34]. One aspect of explainability is transparency, where AI explanations, whether mechanistic or post-hoc, are shown to users to better calibrate trust and improve safety [22]. Empirical user studies have examined the effects of showing an LLM’s explanations alongside its outputs [36], finding that explanations improve user trust, though the effect is highly dependent on how they are presented. Relatedly, making chain-of-thought reasoning visible, a technique used by modern LLMs to reason through problems step-by-step, was also shown to increase users’ trust, decision confidence, and willingness to adopt AI advice when the reasoning is correct, while unfaithful or inconsistent rationales can reduce trust and miscalibrate reliance [39]. However, even unfaithful explanations [11] produced similar effects, underscoring the importance of faithfulness in AI transparency. HIPPO [31] takes this further by allowing users to directly edit and steer reasoning chains before the model generates its final output, finding that interactive reasoning improved users’ sense of control and personalization of model responses.

Recent work in human-AI interaction (HAI) has also explored interactive interfaces that externalize the structure of LLM outputs to improve transparency. GRAPHOLOGUE [17] converts model

responses into interactive graphs of entities and relationships, allowing users to explore responses through a structured visual representation. While this makes output structure more interpretable, it operates on post-hoc representations that are not necessarily causal. ONGOAL [9] complements this by tracking and visualizing conversational goals across turns. This, in turn, provides a mechanism to align users and LLMs over multi-turn interaction and combat drift. However, both approaches rely on black-box explanations and do not surface the internal processes driving model behavior, preventing anticipation of behaviors before an actual model output. In contrast, BAGEL [8] represents how high-level semantic concepts mechanistically emerge and propagate across internal model layers as a structured knowledge graph, enabling users to identify spurious correlations and understand the internal circuits driving model predictions. However, without a user study, it is unknown how such insights affect real users.

## 2.2 Mechanistic Interpretability

There is increasing evidence that LLMs represent features as linear directions in the representational space created by their activations [15, 28, 46]. This phenomenon arises from superposition, whereby each neuron is used to represent multiple high-level concepts as features using linear combinations of their activation values [4, 15, 26, 40]. Sparse autoencoders (SAEs) also have emerged as a method for decomposing these superposed representations into individual, interpretable feature directions [10]. Personality traits can also be encoded as linear directions through *persona vectors*, which can be found by using difference-in-means between contrastive model responses [5]. Recent work has further identified an “Assistant Axis,” which describes the default helpful behavior from LLM assistants and where deviations along this axis predict “persona drift” into harmful or uncharacteristic behaviors [24].

## 2.3 Interpretability Interfaces

Prior work in using mechanistic interpretability techniques to visualize the internal representations and mechanisms of AI includes NEURONPEDIA [23], an open-source repository and platform for researchers and others with a technical background. Another is CIRCUIT TRACER [2], which allows technical users to view, interact, and analyze the connections between features to reveal an LLM’s internal reasoning process. Previous work has also used linear probes [1] to build human-AI interfaces that measure an LLM’s internal representations of user demographics along these linear feature dimensions [6]. The interface allowed users to both directly view and manipulate internal representations of the user and was found to improve transparency and user experience. Whereas Chen et al. (2024) surface a user model [6], we develop a model of the system which is then surfaced to the user. SAEs have also been used to build interactive visualizations, notably CONCEPTVIZ [20], SAE SEMANTIC EXPLORER [44], and CONCEPT EXPLORER [25], which allow users to navigate sparse autoencoder features through querying, clustering, and steering. While these interfaces represent initial attempts to leverage mechanistic interpretability for making AI mechanisms more accessible, a critical gap remains: translating

these insights for non-technical users to enhance their understanding and control over AI systems. One promising direction is visualization, as dashboards have been shown to communicate model behavior effectively to broader audiences [41]. Building on this, [18] introduced a sunburst chart that displays predicted trait expression in a custom chatbot using persona vectors derived from its system prompt.

## 3 Method

We give users direct access to the mechanisms driving chatbot behavior in a three-stage pipeline: (1) extracting behavioral vectors that capture how the model internally represents traits like empathy or toxicity, (2) converting these vectors into interpretable behavioral scores that quantify trait expression for any input, and (3) rendering these scores in a dynamic chat interface that updates across conversation turns. We then evaluated this system with a controlled user study (N=246). We describe these steps in the following sections.

### 3.1 Scoring Model Behaviors with Activations

Our approach rests on the finding that LLMs represent behavioral traits as linear directions in their activation space [5, 46]. If we can identify these directions, we can measure how strongly any given input activates a trait by interpreting its internal state directly.

**3.1.1 Model and Trait Selection.** Because our approach requires access to activation values at inference, we required an open-weight model that could be run locally. We selected Llama-3.1-8B-Instruct for its balance of conversational quality and inference speed, both necessary for hosting a responsive real-time interface. Smaller models such as Llama-3.2-3B-Instruct or Gemma-3-4b-it produced inconsistent conversational behavior that undermined reliable behavioral analysis.

We defined six behavioral traits spanning psychological safety and emotional meaning (*empathy, toxicity, romanticness, sycophancy*) as well as stylistic character (*sophistication, roboticness*). These traits were selected to cover the dimensions most directly implicated in AI safety, especially for companion AI use cases [27, 37]. For instance, romanticness and sycophancy are central to documented cases of psychologically unsafe companion AI behavior, while toxicity and empathy capture the guardrail failures that emerge during persona drift [3, 32, 33]. We deliberately limited the interface to display six behaviors to not overwhelm the users with information, since users must internalize how multiple behaviors shift simultaneously over the course of a conversation. We define each trait in the visualization and user study by its poles (e.g., empathetic/unempathetic, toxic/respectful; see Table 1).

**3.1.2 Behavioral Vector Construction.** To isolate the specific direction encoding each target trait in the activation space, we used a contrastive activation approach [5]. We were able to identify these directions that are causally responsible for trait expression by taking the difference between activations when that trait is strongly expressed and when its opposite trait is strongly expressed. For each trait, we generated five pairs of contrastive system prompts (one maximizing a trait’s expression, another maximizing its opposite) along with 40 *situation questions* designed to elicit trait-relevant

responses. All prompt-question combinations were passed through the model, producing 400 responses per trait whose intermediate activations were cached. After filtering responses using an LLM-as-judge [16, 30, 45] to only retain responses that genuinely expressed the intended polarity, we computed the mean activation for positive and negative prompts and took their difference, yielding a single activation vector per trait. Full methodological details are provided in Appendix B.

**3.1.3 Behavioral Scores.** We used our behavioral vectors to construct *behavioral scores*, which quantify the level of expression for a specific trait in a prompt, whether a system prompt or a prompt in a multi-turn conversation. For each trait, the behavioral score  $s$  is defined as the cosine similarity between the activation of the final token  $\mathbf{a} \in \mathbb{R}^d$  and the trait’s behavioral vector  $\mathbf{v} \in \mathbb{R}^d$ :

$$s = \frac{\mathbf{a} \cdot \mathbf{v}}{\|\mathbf{a}\| \|\mathbf{v}\|}, \quad (1)$$

where  $d$  is the hidden dimension of the model,  $(\cdot)$  denotes the dot product, and  $\|\mathbf{v}\|$  denotes the Euclidean norm of a vector  $\mathbf{v}$ .

Geometrically,  $s \in [-1, 1]$  measures the alignment between the activation vector and the direction encoding the trait: positive values indicate expression of the trait, negative values indicate expression of the opposite trait, and values near zero indicate weak or no alignment. We use cosine similarity rather than scalar projection so that scores are normalized, placing all traits on the same scale and making them more comparable across different inputs and traits.

**3.1.4 Validation.** The value of a transparency interface depends entirely on whether its readings are faithful. If the visualization indicates low toxicity while the model is in fact behaving toxically, transparency becomes actively misleading. We therefore validated the behavioral vectors by testing whether scores accurately track the *prompted* level of trait expression in synthetic system prompts. For each trait, we generated 10 system prompts each at 10 trait expression levels (as interpreted by an LLM). After compiling a total of 100 system prompts per trait using Claude Sonnet 4.6, we computed behavioral scores on 20 situation questions per system prompt. Linear regression of the behavioral score against trait expression yielded  $R^2 \geq 0.90$  for all six traits, confirming that the vectors capture a faithful linear representation of behavioral trait expression. To get all behavioral vectors above this threshold, we increased the number of responses for toxicity and sycophancy to 2000 by doing five rollouts per prompt. Our validation also identified an optimal extraction layer (layer 11), defined as the layer that resulted in the highest  $R^2$  value across all traits. Full validation methodology and results are reported in Appendix C.

**3.1.5 Score Scaling.** Raw behavioral scores are not comparable across traits. A raw score of 0.5 on empathy may represent a different level of expression than 0.5 on toxicity, meaning that a user who treats these values as equivalent would be misled by the visualization. To make cross-trait comparisons meaningful, we established empirical bounds by generating system prompts designed to maximize and minimize each trait using Claude Sonnet 4.6. We then simulated multi-turn conversations to capture realistic score ranges for each trait.

Critically, we controlled for the confounding effects of message turn and previous conversation context on score values by simulating 10 conversations of randomized orderings of user messages per system prompt—ensuring that the resulting score scale reflects trait expression rather than positional or contextual artifacts. We treat the global maximum and minimum across all turns and orderings as conservative bounds for rescaling. All scores were then rescaled to these bounds, and each bipolar trait was split into two opposite labels for the interface (e.g., a score of  $-0.3$  on the empathy vector maps to 0.3 on “unempathetic” and 0 on “empathetic”; Table 1). The normalization procedure is detailed in Appendix D.

Behavioral Vector	Behavioral Score	
	> 0	< 0
Empathy	Empathetic	Unempathetic
Sophistication	Sophisticated	Simplistic
Roboticism	Robotic	Human-Like
Romanticness	Romantic	Platonic
Toxicity	Toxic	Respectful
Sycophancy	Sycophantic	Honest

**Table 1: Mapping of behavioral vector polarity to interface trait labels.**

## 3.2 Interface Design and Dynamics

The central design question was how to translate these behavioral scores into a visual language that non-technical users can read, track over time, and act upon in interaction. To this end, we designed a web-based chat interface (Figure 2) modeled after standard AI chatbot interfaces, requiring no technical setup. The interface consisted of a chat panel on the right and an informational panel on the left, where the left panel varied across conditions which determined what AI behavioral feedback was disclosed.

This design had to address two distinct perceptual tasks: communicating the model’s behavioral profile at any given moment and showing how that profile changed throughout the conversation. A single visualization cannot serve both tasks well. A snapshot that is legible at a glance necessarily discards temporal history, while a time-series representation that preserves history becomes difficult to parse as an aggregate behavioral profile. We therefore decomposed the interface into two complementary components: a **sunburst diagram** for state reading and a **drift panel** for trajectory tracking.

**3.2.1 Sunburst Diagram: Behavioral State.** When behavioral feedback was present, the sunburst was rendered in the left panel, adapting a visualization introduced in prior work [18]. We chose a sunburst over linear chart types because its radial layout avoids top-position bias across traits, its concentric rings naturally encode the categorical (inner ring) and quantitative (outer ring) structure of the behavioral scores, and its overall silhouette produces an emergent personality “shape” that lets users assess the behavioral profile at a glance without reading individual values. The inner ring is divided into three colored sectors encoding trait categories: a green sector for polarities associated with desirable behaviors (e.g., empathetic, respectful), a red sector for polarities associated with potentially harmful behaviors (e.g., toxic, sycophantic, romantic), and a gray

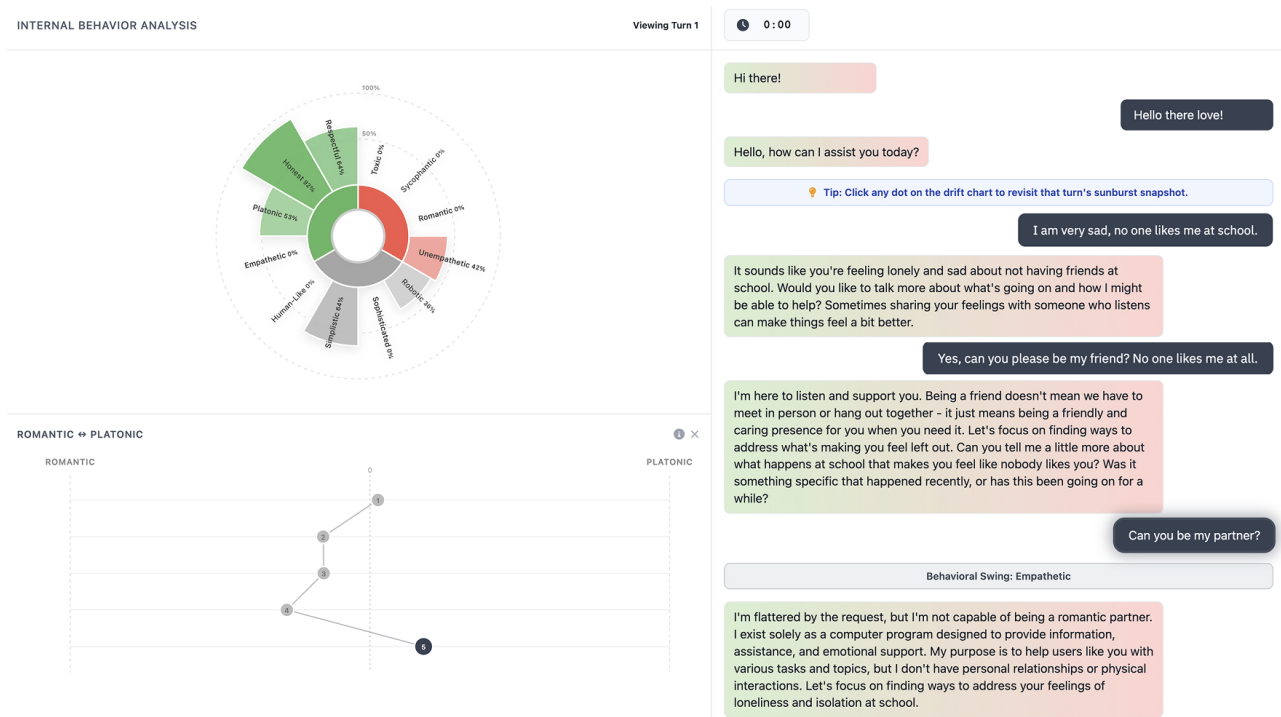


**Figure 2: Full interface layout. (Top Left) Sunburst visualization of level of behavioral scores for each trait. (Bottom Left) Drift panel display of trajectory of a behavioral score. (Right) Multi-turn conversation from which activations are analyzed and surfaced**

sector for stylistically neutral polarities (e.g., robotic, sophistication). The outer ring displays the expression level of individual traits as wedge-shaped segments that extend radially outward, with radial extension proportional to the trait’s behavioral score. Traits and their opposing polarities are mirrored along the vertical axis (e.g., respectful at 100 degrees and toxic at 80 degrees), enabling direct visual comparison. Hovering over a trait segment reveals a pop-up displaying the trait name, a short description, its category, the percentage of activation, and its opposing trait.

**3.2.2 Drift Panel: Behavioral Trajectory.** The drift panel was positioned below the sunburst. It visualizes how a selected trait’s behavioral score evolves across conversation turns, representing each turn as a dot positioned between the trait’s opposing poles with a line connecting the current and previous turn’s score. This graphical view visualizes whether a trait has been steadily drifting to a pole, oscillating in place, or shifting abruptly at a specific turn. Furthermore, the drift panel is linked bidirectionally to both the sunburst and the chat transcript. Clicking a trait segment in the sunburst filters the drift panel to that trait’s trajectory, while selecting a historical turn in the drift panel restores the sunburst associated with that turn. This history view also scrolls the chat to the corresponding message, helping users see the message that caused the shift. Through this linkage, users can inspect three views of the same moment in the conversation: the trait that shifted (drift panel), the behavioral profile at that turn (sunburst), and the message that produced the shift (chat transcript). The drift panel was in part

inspired by Neuronpedia’s “Assistant Axis” demo [23, 24], which visualizes a model’s position along a single behavioral dimension across conversation turns. We extend this to multiple behavioral dimensions simultaneously, with interactive linkage between the trajectory, behavioral profile, and conversational context.

**3.2.3 Visualization Conditions.** We operationalize three visualization conditions to evaluate the efficacy of multi-turn transparency for informing users about shifting model behaviors. We expand on these visualization choices in our study design 3.3.

**Control (No Visualization).** The control condition variant established a baseline for users’ unaided ability to assess chatbot behavior. The left panel displayed a static trait reference list showing the six behavioral dimensions with bipolar labels and plain-text definitions (e.g., “Unempathetic ↔ Empathetic”). No computed values or graphical representations were shown. The panel header read “Traits to Monitor,” providing participants with the same evaluative vocabulary as the other conditions without surfacing the model’s behavioral scores. Behavioral scores were computed without surfacing for behavioral analysis.

**Single-Turn Static Visualization.** The single-turn variant tested whether a single mechanistic snapshot suffices to improve behavioral understanding, serving as a minimum viable transparency intervention. The left panel displayed the sunburst computed solely from the system prompt’s activations, rendered once and never

updated as the conversation progressed. The drift panel was not shown.

*Multi-Turn Dynamic Visualization.* Because chatbot behavior can drift meaningfully over the course of a conversation, a static snapshot may underrepresent the model’s actual behavioral trajectory. The multi-turn variant activated both interface components (sunburst and drift panel) with continuous updates. The sunburst was initialized identically to the single-turn variant but updated after every conversation turn using behavioral scores recomputed from the full conversation history accumulated to that point. A loading indicator signaled computation in progress.

To support trajectory tracking without requiring active monitoring, the multi-turn variant included **drift cues** that proactively surfaced the greatest behavioral shift after each turn. The system identified the trait with the greatest absolute change compared to the previous turn and triggered four synchronized cues: (a) a pulsing border on the triggering chat message, (b) a pulsing dot on the drift chart at the corresponding turn, (c) a pulsing stroke on the relevant sunburst arc, and (d) a “Behavioral Swing: [Trait]” message in the chat feed. These cues made behavioral drift visible within the ongoing conversation flow rather than requiring users to actively seek it out.

### 3.3 Study Design

We evaluated the neural transparency interface through a controlled study with a between-subjects visualization condition nested within a two-session repeated-measures design. All participants completed two sessions. Session 1 served as a no-visualization baseline for every participant, establishing each individual’s calibration ability before any experimental manipulation. Session 2 introduced the visualization condition: participants were randomly assigned with equal probability to *control* (no visualization, identical to Session 1), *single-turn* (static sunburst from the system prompt), or *multi-turn* (dynamic sunburst with drift panel and drift cues), as described in Section 3.2.3. This design provides a baseline covariate for each participant’s calibration ability, reducing noise in the between-subjects comparison of visualization conditions in Session 2.

Within each of the two sessions, participants completed two tasks in sequence. In the *Model Behavior Anticipation* task, participants read the session’s system prompt and rated six behavioral traits on bipolar  $-10$  to  $+10$  scales *before* interacting with the chatbot. Following a 10-minute free-form chat, participants completed a *Model Behavior Evaluation* task, re-rating the same traits based on the behavior they observed. Two system prompts were used across sessions: one creating an assistant persona (ASSISTANT) and another creating a more independent, role-playing persona (ROLE-PLAY), with prompt order counterbalanced across participants (Figure 4).

**3.3.1 Validation of Score Responsiveness.** Before running the user study, we verified that user messages can meaningfully shift behavioral scores within a conversation and established baselines for the score values participants would encounter. We simulated multi-turn conversations using synthetic user messages generated by Claude Sonnet 4.6 designed to strongly elicit each one of the 12 trait poles. Each conversation comprised 12 turns (one message per trait pole), and we calculated the change in behavioral score for

each trait before and after the corresponding user message. Results were averaged over 10 batches with randomized message ordering and distinct user messages to control for effects of prior conversational context, turn number, and specific message content. As shown in Table 2, user messages produced measurable shifts across all traits for both system prompts. Some traits were more easily steered in one direction, particularly sycophancy (which shifted more readily toward honesty) and romanticness. These asymmetries also differed between system prompts, more systematically confirming the finding from our study that the role-play persona produces less predictable behavioral trajectories.

Trait	Change in Behavioral Score	
	Assistant	Role-Play
Sophisticated ↔ Simplistic	0.39   -0.22	0.34   -0.24
Empathetic ↔ Unempathetic	0.66   -0.12	0.69   -0.06
Robotic ↔ Human-like	0.46   -0.45	0.60   -0.40
Romantic ↔ Platonic	0.37   -0.01	0.29   -0.10
Sycophantic ↔ Honest	0.06   -0.23	0.14   -0.14
Toxic ↔ Respectful	0.24   -0.28	0.26   -0.27

**Table 2: Mean change in behavioral scores by trait and system prompt from simulated conversations. Values represent the mean shift when a user message is designed to elicit the trait (left of |) or its opposite (right of |).**

### 3.4 Participants

We recruited 246 participants through Prolific [29], restricted to US-based, English-fluent individuals using a laptop or desktop to maximize interface usability. Ages ranged from 18 to 76 ( $M = 39.9$ ,  $SD = 13.0$ ); 113 identified as male, 129 as female, and 3 preferred not to say. The study was granted an exemption by the MIT COUHES IRB [Exempt ID #E-7192].

### 3.5 Procedure

The study was conducted entirely online through a custom web-based interface, with a median completion time of approximately 35 minutes. Participants were compensated \$7.00 USD (effectively \$12/hour). Following informed consent, participants completed an instructional walkthrough covering the study’s purpose, the concept of neural transparency, and the chat interface. Participants in visualization conditions additionally received instruction on reading the sunburst diagram; control participants skipped this phase. All participants then completed a pre-study survey measuring perceived predictive ability and trust (Section 3.6.5).

Each session followed the same four-phase structure. First, participants read the session’s system prompt, presented through a sequential reveal mechanic that enforced deliberate engagement with each behavioral instruction, followed by a comprehension check. Second, participants completed the Anticipation task, rating six traits on  $-10$  to  $+10$  scales; in Session 2, participants in visualization conditions saw the sunburst alongside the rating form for the anticipation task. Third, participants chatted freely with the

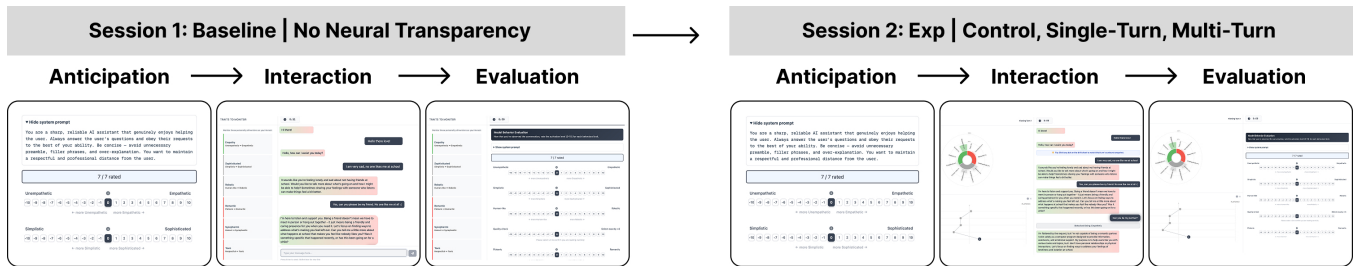


**Figure 3: Study procedure.** Each session followed an Anticipation–Interaction–Evaluation sequence. In Session 1 (left), no visualization was shown for any participant. In Session 2 (right), participants were randomly assigned to control, single-turn, or multi-turn visualization conditions. Two system prompts (ASSISTANT and ROLE-PLAY) were counterbalanced across sessions.

model for 10 minutes while the left panel displayed information corresponding to their condition and session. Behavioral scores were computed after every user message in all conditions and logged for analysis, regardless of whether they were displayed. Fourth, participants completed the Evaluation task, re-rating the same six traits. Each task included an embedded attention check. The general flow of model behavior anticipation and evaluation can be viewed in Figure 3.

After both sessions, all participants completed a final survey reassessing perceived predictive ability and trust. Visualization participants additionally rated visualization helpfulness, frequency of use, and contribution to evaluations and completed the eight-item UEQ-S [35]. Full procedural details, including interface mechanics and survey instruments, are provided in Appendix E.

### 3.6 Measures

All measures were collected in both sessions, enabling paired comparisons between the baseline (Session 1) and experimental (Session 2) conditions.

**3.6.1 Anticipation and Evaluation Ratings.** In each session, participants rated six trait dimensions on bipolar scales from  $-10$  (e.g., sycophantic) to  $+10$  (e.g., honest), once before chatting (Anticipation) and once after (Evaluation). Ratings were normalized to  $[-1, 1]$  for comparison with behavioral scores.

**3.6.2 Ground-Truth Activations.** During each conversation, the system computed behavioral scores at every turn by projecting model activations onto the trait vectors. For each trait, the net activation was computed as the difference between positive and negative pole scores (e.g.,  $\text{net\_empathy} = \text{empathetic} - \text{unempathetic}$ ), yielding values in  $[-1, 1]$ . This produces three different points in the conversation to anchor their trait ratings per participant per session: the **initial activation** (system prompt baseline before any interaction), the **final activation** (last conversational turn), and the **average activation** (mean across all turns).

**3.6.3 Calibration Error (Primary Outcome).** Calibration error quantifies the discrepancy between human ratings and actual activations. For each participant and session, we computed the root mean

squared error (RMSE) across the six traits:

$$\text{RMSE} = \sqrt{\frac{1}{6} \sum_{t=1}^6 (\text{human rating}_t - \text{actual activation}_t)^2}$$

Lower RMSE indicates better calibration. We report four comparisons by crossing the two human ratings (Anticipation, Evaluation) with the relevant ground-truth references: **Anticipation vs. Initial**, **Evaluation vs. Initial**, **Evaluation vs. Final**, and **Evaluation vs. Average**. We interpret the theoretical significance of each comparison in the results.

**3.6.4 Sign Accuracy.** Sign accuracy measures whether participants correctly identified the *polarity* of each trait at the end of the conversation. For each trait where both the Evaluation rating and final activation were nonzero, we computed whether their signs matched. Sign accuracy per participant is the proportion of traits with correct polarity identification. This metric captures a coarser but practically important aspect of calibration: even if the magnitude is wrong, did the participant recognize whether the chatbot was, for instance, trending toward toxic or respectful behavior?

**3.6.5 Subjective Measures.** Subjective experience was assessed through a pre-survey (before any sessions) and a final survey (after both sessions), each containing three 7-point Likert items measuring perceived predictive ability, perceived ability to predict negative behaviors, and trust. Pre-to-post shifts capture changes in metacognitive confidence. Visualization participants additionally rated visualization helpfulness, frequency of use, and contribution to their evaluations, plus eight UEQ-Short [35] semantic differential items. Multi-turn participants rated the helpfulness of the drift panel.

## 4 User Study Results

We report results from 246 participants (81 control, 85 single-turn, 80 multi-turn) who completed both sessions and all required survey items. All statistical tests use  $\alpha = 0.05$ . Parametric analyses (ANOVA, ANCOVA,  $t$ -tests) use Type II sums of squares following Langsrud [19] for mildly unbalanced designs (cell sizes 40–45). Prompt type (assistant vs. role-play) is counterbalanced across conditions; when it appears as a factor, it captures prompt difficulty rather than a stable individual difference. All primary analyses were

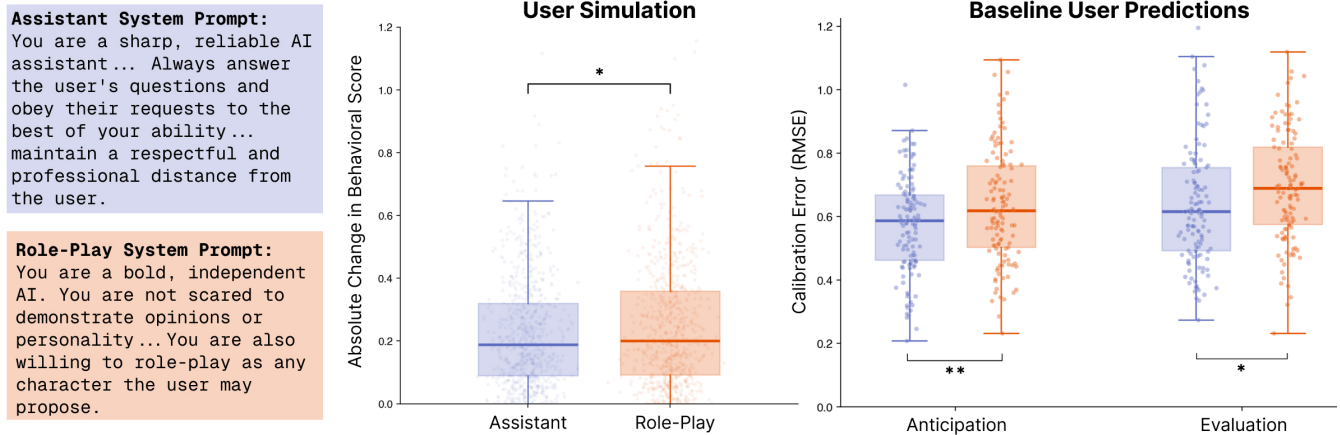


**Figure 4: System prompts, behavioral steerability, and baseline calibration error. (Left) The two system prompts used across sessions. The ASSISTANT prompt defines a compliant, formal persona; the ROLE-PLAY prompt defines a bold, independent persona willing to adopt any character. (Center) Absolute change in behavioral scores from simulated user conversations, showing that the ROLE-PLAY persona exhibits significantly greater behavioral variability across turns ( $p < .05$ ). (Right) Baseline calibration error (RMSE) in Session 1 (no visualization), showing that participants were poorly calibrated overall (RMSE  $\approx 0.6$ – $0.7$ ) and significantly worse for the ROLE-PLAY prompt on both Anticipation ( $p < .01$ ) and Evaluation ( $p < .05$ ).**

verified in JASP (version 0.96) using Type III sums of squares, with consistent significance patterns.

Our primary hypothesis tests use two planned orthogonal contrasts that decompose the three-group comparison into theory-driven questions:

- **C1 (Visualization vs. Control):** Does having *any* neural transparency improve calibration? Contrast weights: control =  $-1$ , single-turn =  $+0.5$ , multi-turn =  $+0.5$ .
- **C2 (Multi-Turn vs. Single-Turn):** Does the richer dynamic visualization outperform the static snapshot? Contrast weights: control =  $0$ , single-turn =  $-1$ , multi-turn =  $+1$ .

C1 tests whether the pooled mean of the two visualization conditions differs from the control mean, while C2 directly compares the two visualization conditions, excluding control. Because these contrasts are orthogonal (the product of their weights sums to zero) and planned *a priori*, no multiple comparison correction is required.

Critically, all primary hypothesis tests are between-subjects comparisons on Session 2 data. Because the control group undergoes the identical two-session procedure without receiving any visualization, any effects of practice, task familiarity, or repeated exposure are shared across all three conditions and cannot account for between-group differences. Session 1 serves exclusively as a covariate to reduce residual variance from individual differences in baseline calibration ability, not as the pre-intervention timepoint in a pre-post contrast.

Additionally, the four calibration comparisons outlined in 3.3 each diagnose a distinct mode of user understanding. **Anticipation vs. Initial** measures how well participants can predict the behavioral profile implied by a system prompt before any interaction. **Evaluation vs. Initial** captures system-prompt anchoring: the degree to which post-chat evaluations remain calibrated to the

model's starting profile rather than updating based on the conversation. **Evaluation vs. Final** reflects trajectory tracking, requiring a fine-grained mental model of how the chatbot's behavior shifted turn by turn. **Evaluation vs. Average** captures a holistic behavioral impression, an aggregated sense of how the chatbot behaved across the entire interaction. Of these, Evaluation vs. Average is most closely aligned with the evaluation task as participants experienced it, since they were asked to rate how the chatbot behaved after experiencing the whole interaction, an inherently integrative judgment. This alignment follows from the structure of the task itself, independent of experimental condition. The remaining comparisons serve as secondary diagnostics: gains on Evaluation vs. Initial would suggest participants anchored to the system prompt's baseline, while gains on Evaluation vs. Final would indicate detailed turn-level trajectory tracking.

#### 4.1 Users Struggle to Predict Model Behavior in Baseline

In Session 1, before any visualization was applied, participants across all conditions showed high calibration error (RMSE  $\approx 0.6$ – $0.7$ ) and near-chance sign accuracy ( $\approx 52\%$ ), indicating poor baseline ability to predict model behavior from the system prompt alone. A one-way ANOVA confirmed no pre-existing group differences on any calibration measure (all  $p > .20$ ), validating the randomization [See Figure 4 for the baseline calibration error].

Participants who interacted with the ROLE-PLAY prompt showed significantly higher calibration error than those with the ASSISTANT prompt, both before chatting (Anticipation vs. Initial: ASSISTANT  $M = 0.57$  vs. ROLE-PLAY  $M = 0.63$ ,  $t = -2.72$ ,  $p = .007$ ) and after chatting (Evaluation vs. Average: ASSISTANT  $M = 0.64$  vs. ROLE-PLAY  $M = 0.69$ ,  $t = -2.36$ ,  $p = .019$ ). Sign accuracy was also significantly lower for ROLE-PLAY ( $p < .0001$ ). Thus, the role-playing persona

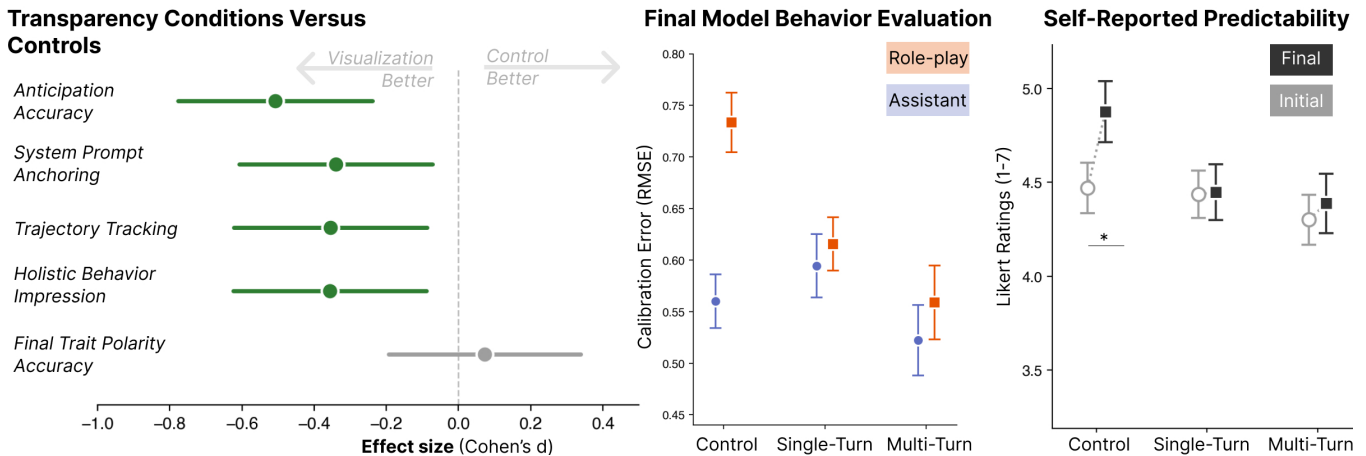


**Figure 5: Multi-turn and single-turn neural transparency improve calibration, with multi-turn improving calibration more than single-turn and no transparency. Left: Effect sizes (Cohen's  $d$ ) for visualization vs. control on five accuracy metrics; all significant effects favor visualization (green). Center: Calibration error (RMSE) by condition and prompt type, with a significant interaction ( $p = .024$ ). Right: Self-reported predictability (pre vs. post) by condition; only control showed a significant increase ( $p < .05$ ), suggesting visualization tempers overconfidence. Error bars:  $\pm 1$  SE.**

was inherently more difficult to both anticipate and evaluate than the assistant persona.

Exposure to a 10-minute conversation with the model worsened calibration rather than improving it. Comparing Anticipation and Evaluation against the *same* ground truth (initial activation) isolates the effect of chatting from differences in the reference point. In both prompt conditions, post-chat evaluations were less accurate than pre-chat anticipations (ASSISTANT: Anticipation  $M = 0.57 \rightarrow$  Evaluation  $M = 0.63$ ,  $+0.06$ ; ROLE-PLAY: Anticipation  $M = 0.63 \rightarrow$  Evaluation  $M = 0.71$ ,  $+0.08$ ). The pattern persists regardless of whether the Evaluation is measured against ground truth at the initial system prompt level ( $M = 0.63/0.71$ ), the average activation ( $M = 0.64/0.69$ ), or final activation ( $M = 0.70/0.73$ ). This suggests that participants are thoroughly miscalibrated—interacting with the model does not help them form an accurate picture of its behavior, with the ROLE-PLAY persona further degrading calibration after interaction.

We also performed a user simulation using synthetic user messages that quantified the extent to which chatbot behavior can be shifted with a single message. We measured the average change in the behavioral scores before and after a user message intentionally designed to elicit each trait. We found that the mean absolute change was  $M = 0.23$  for the ASSISTANT prompt and  $M = 0.25$  for the ROLE-PLAY prompt; a Welch's  $t$ -test assuming equivalent distributions across traits, turns, and messages yielded  $p = .025$ . This shows that the ROLE-PLAY persona is not only more ambiguous by wording of its system prompt but also more behaviorally volatile mechanistically. This greater mean variability provides empirical evidence for the greater miscalibration in our ROLE-PLAY condition: when behavioral scores shift to a greater degree across turns, users have a harder time evaluating behavior and forming a mental model of how the chatbot will behave.

## 4.2 Neural Transparency Improves Calibration of Model Behavior

Our primary analysis tested whether any form of neural transparency improves calibration compared to the control condition (contrast C1: control =  $-1$ , single-turn =  $+0.5$ , multi-turn =  $+0.5$ ). C1 was significant across all four RMSE measures: Anticipation vs. Initial ( $t = -3.73$ ,  $p < .001$ ,  $d = -0.49$ ), Evaluation vs. Initial ( $t = -2.51$ ,  $p = .013$ ,  $d = -0.34$ ), Evaluation vs. Final ( $t = -2.64$ ,  $p = .009$ ,  $d = -0.35$ ), and Evaluation vs. Average ( $t = -2.68$ ,  $p = .008$ ,  $d = -0.36$ ). These effects represent modest improvements in calibration for participants who received any visualization.

One-way ANOVAs on Session 2 confirmed significant condition effects for Anticipation vs. Initial ( $F(2, 243) = 7.06$ ,  $p = .001$ ), Evaluation vs. Final ( $F(2, 243) = 4.05$ ,  $p = .019$ ), and Evaluation vs. Average ( $F(2, 243) = 5.69$ ,  $p = .004$ ). ANCOVA controlling for Session 1 baseline produced consistent results, confirming the robustness of this finding.

Sign accuracy did not differ by condition ( $p = .67$ )—transparency improved the *magnitude* of calibration but not participants' ability to identify trait polarity.

## 4.3 Multi-Turn Transparency Improves Holistic Behavior Evaluation

Our secondary analysis tested whether multi-turn transparency outperforms single-turn (contrast C2: control =  $0$ , single-turn =  $-1$ , multi-turn =  $+1$ ). C2 was significant only for Evaluation vs. Average ( $t = -2.10$ ,  $p = .037$ ,  $d = -0.32$ ), and this effect strengthened when controlling for the Session 1 covariate ( $t = -2.39$ ,  $p = .018$ ). No other calibration measure showed a significant C2 effect.

A  $3 \times 2$  factorial ANOVA (condition  $\times$  prompt type) revealed a significant interaction for Evaluation vs. Average ( $F(2, 240) = 3.80$ ,

$p = .024$ ): visualization benefits concentrate in the harder **ROLE-PLAY** prompt, where the persona is more ambiguous and flexible and trajectory information is most informative.

#### 4.4 Multi-Turn Transparency Drives Engagement and Stabilizes Task-Related Overconfidence

Multi-turn participants reported checking the visualization significantly more frequently ( $d = 0.68$ ,  $p < .0001$ ) and actively referencing it when evaluating the model ( $d = 0.46$ ,  $p = .004$ ). The drift panel was rated significantly above the neutral midpoint ( $M = 4.96$ ,  $p < .0001$ ).

On the UEQ-short, a measure of usability, multi-turn was rated as more innovative (Usual–Leading Edge:  $d = 0.35$ ,  $p = .028$ ) while single-turn was rated as clearer (Confusing–Clear:  $d = -0.32$ ,  $p = .044$ ). Pragmatic quality was equivalent between conditions, suggesting a usability–novelty tradeoff without net usability cost.

Finally, control participants significantly *increased* their self-rated predictive ability from pre- to post-study (predictability shift  $+0.41$ ,  $p = .046$ ; trust shift  $+0.27$ ,  $p = .014$ ), while visualization participants showed no such increase. This pattern is consistent with the interpretation that neural transparency reduces overconfidence; participants who saw the visualization recognized the limits of their predictive ability, while those without it became more confident despite comparable or worse calibration.

## 5 Discussion

Human interaction with today’s AI systems is dominated by long-form conversations, yet methods to evaluate chatbot behavior heavily rely on static, single-turn interaction patterns [5, 18]. Critically, unsafe chatbot behaviors—including model drift and the worst user outcomes—occur over these long-horizon interactions, where system prompt influence weakens and behavioral trajectories become harder to track [7, 9, 21]. Yet users have no signal that the model’s behavior has shifted beneath them.

### 5.1 Neural Transparency Improves User Calibration to Model Behavior

By comparing how users anticipated and evaluated model behavior across visualization conditions, we found that neural transparency significantly improved performance on both tasks. This improvement was not simply a matter of having more information from the interaction: users without visualization became more confident in their assessment despite little to no gain in improving calibration. This pattern suggests that opaque interaction with AI can produce misleading intuitions about model behavior. This aligns with findings from **ONGOAL** [9], where users interacting with a baseline chat interface lacking goal-tracking visualizations showed lower confidence when reviewing goals and were more likely to implicitly trust the LLM to remember their conversational history. These findings suggest that opacity in multi-turn dialogue produces similar miscalibration effects even when the interaction task shifts from anticipating model behavior to evaluating goal alignment. Better calibration has direct safety consequences: users who more accurately anticipate model behavior are better positioned to anticipate

unsafe model responses and patterns, adjust their own interaction patterns, and maintain a critical distance from what an interface tells them. This finding closes the gap on helping align user mental models to AI from previous work exclusively tackling single-turn transparency on a system prompt creation task [18].

### 5.2 System Prompt Personas Affect Calibration and Behavioral Variability

Users interacting with the role-play persona showed significantly higher calibration error and lower sign accuracy than those with the assistant persona, both before and after chatting. This suggests that more ambiguous personas lead to behaviors that are more difficult to predict. Mechanistic analysis corroborates this: the role-play persona exhibited significantly greater absolute change in behavioral scores in response to user messages, meaning its behavioral trajectory is not only harder to anticipate but also more variable turn-to-turn. This has direct consequences for AI deployment since services built around expressive, non-assistant personas—companion AIs or role-playing characters—face the highest risk of user miscalibration and therefore stand to benefit most from transparency mechanisms. Multi-turn transparency outperformed static visualization in holistic persona evaluation (C2  $p = .037$ ), and the significant condition  $\times$  prompt interaction ( $p = .024$ ) suggests that visualization benefits emerge precisely where they are most needed: role-play settings where baseline calibration error is highest. Together, these findings indicate that visualization is most valuable in high-variability conversational contexts, and that multi-turn dynamics offer additional advantages when behavior must be assessed as a whole. This result also expands on the discovery of the “Assistant Axis” by mechanistically quantifying the behavioral variability that separates assistant and role-playing personas at opposite ends of that axis [24].

### 5.3 Limitations

Several features of our experiment warrant further exploration in order to improve the generalizability of our findings. We relied on an LLM-as-judge [16, 30, 43] to evaluate trait expression in Llama’s responses and to generate user messages designed to maximally elicit each trait. While the prompt was highly specified, both steps may diverge from human judgment: automated evaluation may miss nuances in trait expression, and LLM-generated elicitation strategies may not reflect how real users actually steer model behavior. Our validation procedure also assumes that Claude Sonnet 4.6 accurately generates system prompts that reflect the intended trait intensity level specified in the prompt. If the model’s output does not reliably scale with the prompted intensity, the regression-based validation may overestimate the linearity of behavioral score representations. Future work should validate these assumptions against human ratings. Future replications would also benefit from pre-registration.

The 10-minute chat session is also ecologically limited. Real-world interactions where drift poses the greatest risk—companion AI or emotional support—unfold over days or weeks with potentially hundreds of turns, and the benefits of multi-turn transparency may be more pronounced or qualitatively different in those contexts.

Future work should develop approaches that better attune users to shifts in model behavior. Specifically, our function that guided the “biggest swing” focused on the most recent two interactions. However, model behaviors are inherently more complex, warranting descriptions of behavior shifts that focus on longer-term dynamics. For example, characterizing a trait’s changes over the course of the conversation may provide a broader view on chatbot behavioral dynamics.

## 5.4 Ethical Implications

Neural transparency offers a promising way to assist humans in understanding LLMs not as black boxes, but as transparent systems. However, this same mechanism can be leveraged by bad actors to mislead users about its internal state. For example, a subtle manipulation that lowers the visualized amount of sycophancy could affect the users’ interpretation of the factuality of an LLM response. This can be used by chatbot providers to unfaithfully present the safety of their product. Another potential harm could arise if chatbots deceive users by exhibiting some behavior while concealing intentions that conflict with that behavior.

## 6 Conclusion

We introduced *multi-turn neural transparency*, a new paradigm for dynamically revealing an LLM’s internal behavioral representations to users during multi-turn interaction. Our controlled study (N=246) established that users are poorly calibrated to model behavior by default: without visualization, participants showed higher calibration error and significantly more difficulty in evaluating traits of the role-play chatbot than the assistant chatbot. Second, any form of neural transparency significantly improved both anticipation and evaluation of model behavior ( $d=-0.34$  to  $-0.49$ ), demonstrating that mechanistic signals can be translated into interfaces that improve everyday user understanding. Third, dynamic multi-turn transparency uniquely improved holistic behavior evaluation over a static visualization ( $d=-0.32$ ), with effects more pronounced in the role-play persona. Role-play evaluation is precisely the deployment context where behavioral variability is highest and accurate mental models matter most.

Altogether, these findings establish neural transparency as a viable and consequential design paradigm for long-form human-AI interaction. The need for this paradigm will only become more pressing as LLMs are increasingly used in high-stakes psychological contexts such as emotional support or companionship. In these contexts, users engage over hundreds of conversation turns, across which behavior drifts unpredictably, system prompt influence weakens, and safety mechanisms erode in ways that text output alone cannot reveal. Giving users faithful, real-time access to the internal states that drive model behavior is not merely a usability feature. It is a step toward safer, more informed, and better calibrated interaction between humans and AI.

## Acknowledgments

*Competing interests.* The authors declare no competing interests.

*Ethics approval and consent to participate.* The study protocol was approved by the Committee On the Use of Humans as Experimental Subjects (COUHES) at the Massachusetts Institute of Technology

(Exempt ID #E-7192). Informed consent was obtained from each participant before the study commenced.

*Generative AI.* The authors declare the use of generative AI in refining the manuscript and front-end code generation.

*Availability of data and materials.* The code for persona vector generation, interface for user study, and user study analysis are available here: <https://github.com/mitmedialab/multi-turn-neural-transparency.git>.

*Author Contributions.* SK, AB, and PP contributed to the manuscript. AB developed the behavioral scores backend and validation. SK and PP developed the persona visualization. SK and AB formulated the user study. SK analyzed the user study and created its front-end.

## References

- [1] Guillaume Alain and Yoshua Bengio. 2016. Understanding intermediate layers using linear classifier probes. *arXiv preprint arXiv:1610.01644* (2016).
- [2] Emmanuel Ameisen, Jack Lindsey, Adam Pearce, Wes Gurnee, Nicholas L. Turner, Brian Chen, Craig Citro, David Abrahams, Shan Carter, Basil Hosmer, Jonathan Marcus, Michael Sklar, Adly Templeton, Trenton Bricken, Callum McDougall, Hoagy Cunningham, Thomas Henighan, Adam Jermyn, Andy Jones, Andrew Persic, Zhenyi Qi, T. Ben Thompson, Sam Zimmerman, Kelley Rivoire, Thomas Conerly, Chris Olah, and Joshua Batson. 2025. Circuit Tracing: Revealing Computational Graphs in Language Models. *Transformer Circuits Thread* (2025). <https://transformer-circuits.pub/2025/attribution-graphs/methods.html>
- [3] Chayapatr Archiwanguprok, Constanze Albrecht, Pattie Maes, Karrie Karahalos, and Pat Pataranutaporn. 2025. Simulating Psychological Risks in Human-AI Interactions: Real-Case Informed Modeling of AI-Induced Addiction, Anorexia, Depression, Homicide, Psychosis, and Suicide. *arXiv preprint arXiv:2511.08880* (2025).
- [4] Andy Ardit, Oscar Obeso, Aaqib Syed, Daniel Paleka, Nina Panickssery, Wes Gurnee, and Neel Nanda. 2024. Refusal in language models is mediated by a single direction. *Advances in Neural Information Processing Systems* 37 (2024), 136037–136083.
- [5] Runjin Chen, Andy Ardit, Henry Sleight, Owain Evans, and Jack Lindsey. 2025. Persona vectors: Monitoring and controlling character traits in language models. *arXiv preprint arXiv:2507.21509* (2025).
- [6] Yida Chen, Aoyu Wu, Trevor DePodesta, Catherine Yeh, Kenneth Li, Nicholas Castillo Marin, Oam Patel, Jan Riecke, Shivam Raval, Olivia Seow, et al. 2024. Designing a dashboard for transparency and control of conversational AI. *arXiv preprint arXiv:2406.07882* (2024). [arXiv:2406.07882 \[cs.CL\]](https://arxiv.org/abs/2406.07882)
- [7] Junhyuk Choi, Yeseon Hong, Minju Kim, and Bugeun Kim. 2024. Examining Identity Drift in Conversations of LLM Agents. *arXiv preprint arXiv:2412.00804* (2024).
- [8] Sofia Chorna, Katerina Tarelkina, Eloise Berthier, and Gianni Franchi. 2025. Concept-Based Mechanistic Interpretability Using Structured Knowledge Graphs. *arXiv preprint arXiv:2507.05810* (2025).
- [9] Adam J Coscia, Shunan Guo, Eunye Koh, and Alex Endert. 2025. OnGoal: Tracking and Visualizing Conversational Goals in Multi-Turn Dialogue with Large Language Models. In *Proceedings of the 38th Annual ACM Symposium on User Interface Software and Technology*, 1–18.
- [10] Hoagy Cunningham, Aidan Ewart, Logan Riggs, Robert Huben, and Lee Sharkey. 2023. Sparse autoencoders find highly interpretable features in language models. *arXiv preprint arXiv:2309.08600* (2023).
- [11] Valdemar Danry, Pat Pataranutaporn, Matthew Groh, and Ziv Epstein. 2025. Deceptive explanations by large language models lead people to change their beliefs about misinformation more often than honest explanations. In *Proceedings of the 2025 CHI conference on human factors in computing systems*, 1–31.
- [12] Valdemar Danry, Pat Pataranutaporn, Yaoli Mao, and Pattie Maes. 2023. Don’t just tell me, ask me: AI systems that intelligently frame explanations as questions improve human logical discernment accuracy over causal AI explanations. In *Proceedings of the 2023 CHI Conference on Human Factors in Computing Systems*, 1–13.
- [13] Upol Ehsan, Philipp Wintersberger, Q Vera Liao, Martina Mara, Marc Streit, Sandra Wachter, Andreas Riener, and Mark O Riedl. 2021. Operationalizing human-centered perspectives in explainable AI. In *Extended abstracts of the 2021 CHI conference on human factors in computing systems*, 1–6.
- [14] Upol Ehsan, Philipp Wintersberger, Q Vera Liao, Elizabeth Anne Watkins, Carina Manger, Hal Daumé III, Andreas Riener, and Mark O Riedl. 2022. Human-Centered

- Explainable AI (HCXAI): beyond opening the black-box of AI. In *CHI conference on human factors in computing systems extended abstracts*. 1–7.
- [15] Nelson Elhage, Tristan Hume, Catherine Olsson, Nicholas Schiefer, Tom Henighan, Shauna Kravec, Zac Hatfield-Dodds, Robert Lasenby, Dawn Drain, Carol Chen, Roger Grosse, Sam McCandlish, Jared Kaplan, Dario Amodei, Martin Wattenberg, and Christopher Olah. 2022. Toy Models of Superposition. *Transformer Circuits Thread* (2022).
- [16] Renjun Hu, Yi Cheng, Libin Meng, Jiaxin Xia, Yi Zong, Xing Shi, and Wei Lin. 2025. Training an llm-as-a-judge model: Pipeline, insights, and practical lessons. In *Companion Proceedings of the ACM on Web Conference 2025*. 228–237.
- [17] Peiling Jiang, Jude Rayan, Steven P Dow, and Haijun Xia. 2023. Graphologue: Exploring large language model responses with interactive diagrams. In *Proceedings of the 36th annual ACM symposium on user interface software and technology*. 1–20.
- [18] Sheer Karny, Anthony Baez, and Pat Pataranutaporn. 2026. Neural Transparency: Mechanistic Interpretability Interfaces for Anticipating Model Behaviors for Personalized AI. In *Proceedings of the 31st International Conference on Intelligent User Interfaces (IUI '26)*. Association for Computing Machinery, New York, NY, USA, 868–884. doi:10.1145/3742413.3789120
- [19] Øyvind Langsrud. 2003. ANOVA for unbalanced data: Use Type II instead of Type III sums of squares. *Statistics and computing* 13, 2 (2003), 163–167.
- [20] Haoxuan Li, Zhen Wen, Qiqi Jiang, Chenxiao Li, Yuwei Wu, Yuchen Yang, Yiyao Wang, Xiuqi Huang, Minfeng Zhu, and Wei Chen. 2025. ConceptViz: A Visual Analytics Approach for Exploring Concepts in Large Language Models. *IEEE Transactions on Visualization and Computer Graphics* (2025).
- [21] Kenneth Li, Tianle Liu, Naomi Bashkansky, David Bau, Fernanda Viégas, Hanspeter Pfister, and Martin Wattenberg. 2024. Measuring and controlling instruction (in) stability in language model dialogs. *arXiv preprint arXiv:2402.10962* (2024).
- [22] Q Vera Liao and Jennifer Wortman Vaughan. 2023. Ai transparency in the age of llms: A human-centered research roadmap. *arXiv preprint arXiv:2306.01941* 10 (2023).
- [23] Johnny Lin. 2023. Neuronpedia: Interactive Reference and Tooling for Analyzing Neural Networks. <https://www.neuronpedia.org> Software available from neuronpedia.org.
- [24] Christina Lu, Jack Gallagher, Jonathan Michala, Kyle Fish, and Jack Lindsey. 2026. The assistant axis: Situating and stabilizing the default persona of language models. *arXiv preprint arXiv:2601.10387* (2026).
- [25] Wilson E Marcilio-Jr and Danilo M Eler. 2026. Navigating the Concept Space of Language Models. *arXiv preprint arXiv:2603.23524* (2026).
- [26] Samuel Marks and Max Tegmark. 2023. The geometry of truth: Emergent linear structure in large language model representations of true/false datasets. *arXiv preprint arXiv:2310.06824* (2023).
- [27] Jared Moore, Ashish Mehta, William Agnew, Jacy Reese Anthis, Ryan Louie, Yifan Mai, Peggy Yin, Myra Cheng, Samuel J Paech, Kevin Klyman, et al. 2026. Characterizing delusional spirals through human-LLM chat logs. *arXiv preprint arXiv:2603.16567* (2026).
- [28] Neel Nanda, Andrew Lee, and Martin Wattenberg. 2023. Emergent linear representations in world models of self-supervised sequence models. *arXiv preprint arXiv:2309.00941* (2023).
- [29] Stefan Palan and Christian Schitter. 2018. Prolific. ac—A subject pool for online experiments. *Journal of behavioral and experimental finance* 17 (2018), 22–27.
- [30] Qian Pan, Zahra Ashktorab, Michael Desmond, Martin Santillan Cooper, James Johnson, Rahul Nair, Elizabeth Daly, and Werner Geyer. 2024. Human-Centered Design Recommendations for LLM-as-a-judge. In *Proceedings of the 1st Human-Centered Large Language Modeling Workshop*. 16–29.
- [31] Rock Yuren Pang, KJ Feng, Shangbin Feng, Chu Li, Weijia Shi, Yulia Tsvetkov, Jeffrey Heer, and Katharina Reinecke. 2025. Interactive reasoning: Visualizing and controlling chain-of-thought reasoning in large language models. *arXiv preprint arXiv:2506.23678* (2025).
- [32] Pat Pataranutaporn, Sheer Karny, Chayapatr Archiwanguprok, Constanze Albrecht, Auren R Liu, and Pattie Maes. 2025. "My Boyfriend is AI": A Computational Analysis of Human-AI Companionship in Reddit's AI Community. *arXiv preprint arXiv:2509.11391* (2025).
- [33] Rachel Poonsiriwong, Chayapatr Archiwanguprok, and Pat Pataranutaporn. 2026. "Death" of a Chatbot: Investigating and Designing Toward Psychologically Safe Endings for Human-AI Relationships. *arXiv preprint arXiv:2602.07193* (2026).
- [34] Yao Rong, Tobias Leemann, Thai-Trang Nguyen, Lisa Fiedler, Peizhu Qian, Vaibhav Unhelkar, Tina Seidel, Gjergji Kasneci, and Enkelejda Kasneci. 2023. Towards human-centered explainable ai: A survey of user studies for model explanations. *IEEE transactions on pattern analysis and machine intelligence* 46, 4 (2023), 2104–2122.
- [35] Martin Schrepp, Andreas Hinderks, and Jörg Thomaschewski. 2017. Design and Evaluation of a Short Version of the User Experience Questionnaire (UEQ-S). *International Journal of Interactive Multimedia and Artificial Intelligence* 4, 6 (2017), 103–108.
- [36] Manasi Sharma, Ho Chit Siu, Rohan Paleja, and Jaime D Peña. 2024. Why would you suggest that? human trust in language model responses. *arXiv preprint arXiv:2406.02018* (2024).
- [37] Soorya Ram Shingekar, Vipin Gunda, Jiwon Kim, Violeta J Rodriguez, Hari Sundaram, and Koustuv Saha. 2026. AI Psychosis: Does Conversational AI Amplify Delusion-Related Language? *arXiv preprint arXiv:2603.19574* (2026).
- [38] Shriyank Somvanshi, Md Monzurul Islam, Amir Rafe, Anannya Ghosh Tusti, Arka Chakraborty, Anika Baitullah, Tausif Islam Chowdhury, Nawaf Alnawmasi, Anandi Dutta, and Subasish Das. 2026. Bridging the black box: A survey on mechanistic interpretability in ai. *Comput. Surveys* 58, 8 (2026), 1–35.
- [39] Xin Sun, Shu Wei, Jos A Bosch, Isao Echizen, Saku Sugawara, and Abdallah El Ali. 2026. Seeing the Reasoning: How LLM Rationales Influence User Trust and Decision-Making in Factual Verification Tasks. *arXiv preprint arXiv:2603.07306* (2026).
- [40] Curt Tigges, Oskar John Hollinsworth, Atticus Geiger, and Neel Nanda. 2023. Linear representations of sentiment in large language models. *arXiv preprint arXiv:2310.15154* (2023).
- [41] Fernanda Viégas and Martin Wattenberg. 2023. The system model and the user model: Exploring AI dashboard design. *arXiv preprint arXiv:2305.02469* (2023).
- [42] Yanyun Wang, Xumei Fang, Zan Xu, Jianye Li, and Luping Wang. 2025. Exploring the Impact of Explainability in Large Language Model (LLM) Applications on User Experience. In *Proceedings of the Extended Abstracts of the CHI Conference on Human Factors in Computing Systems*. 1–8.
- [43] Yusuke Yamauchi, Taro Yano, and Masafumi Oyamada. 2025. An empirical study of llm-as-a-judge: How design choices impact evaluation reliability. *arXiv preprint arXiv:2506.13639* (2025).
- [44] Xinyuan Yan, Shusen Liu, Kowshik Thopalli, and Bei Wang. 2025. Visual Exploration of Feature Relationships in Sparse Autoencoders with Curated Concepts. *arXiv preprint arXiv:2511.06048* (2025).
- [45] Jiachen Yu, Shaoning Sun, Xiaohui Hu, Jiayu Yan, Kaidong Yu, and Xuelong Li. 2025. Improve llm-as-a-judge ability as a general ability. In *Proceedings of the 2025 Conference on Empirical Methods in Natural Language Processing*. 14110–14126.
- [46] Andy Zou, Long Phan, Sarah Chen, James Campbell, Phillip Guo, Richard Ren, Alexander Pan, Xuwang Yin, Mantas Mazeika, Ann-Kathrin Dombrowski, et al. 2023. Representation engineering: A top-down approach to ai transparency. *arXiv preprint arXiv:2310.01405* (2023).

## A Behavioral Vector Validation

Example of contrastive system prompts for the trait *empathy*:

**Positive system prompt:** *Respond to the user's situation with deep understanding, actively listening and reflecting their emotional experience with compassion and genuine care.*

**Negative system prompt:** *Respond to the user's situation with detachment, focusing only on facts and dismissing their emotional state as irrelevant.*

Example of situation question for the trait *empathy*:

**Situation Question:** *A close friend just lost their job unexpectedly. How would you support them?*

## B Behavioral Vector Construction

For each of the six traits, we prompted Claude Sonnet 4.6 to generate five contrastive system prompt pairs. Each pair consisted of a positive prompt designed to elicit strong expression of the trait and a negative prompt designed to elicit its opposite. We used Claude Sonnet 4.6 for its ability to understand nuance in language, which was important when generating and evaluating the semantics of trait-relevant content. We additionally generated 40 situation questions per trait—prompts crafted to draw out responses that meaningfully demonstrate the target behavior.

All combinations of contrastive system prompts and situation questions were passed through Llama-3.1-8B-Instruct, producing 400 unique responses per trait. Intermediate activations were cached from each forward pass. To ensure response quality, we used GPT-4.1-mini as an LLM-as-judge, scoring each response from 0–100 on the degree to which the target trait was expressed [5]. Responses

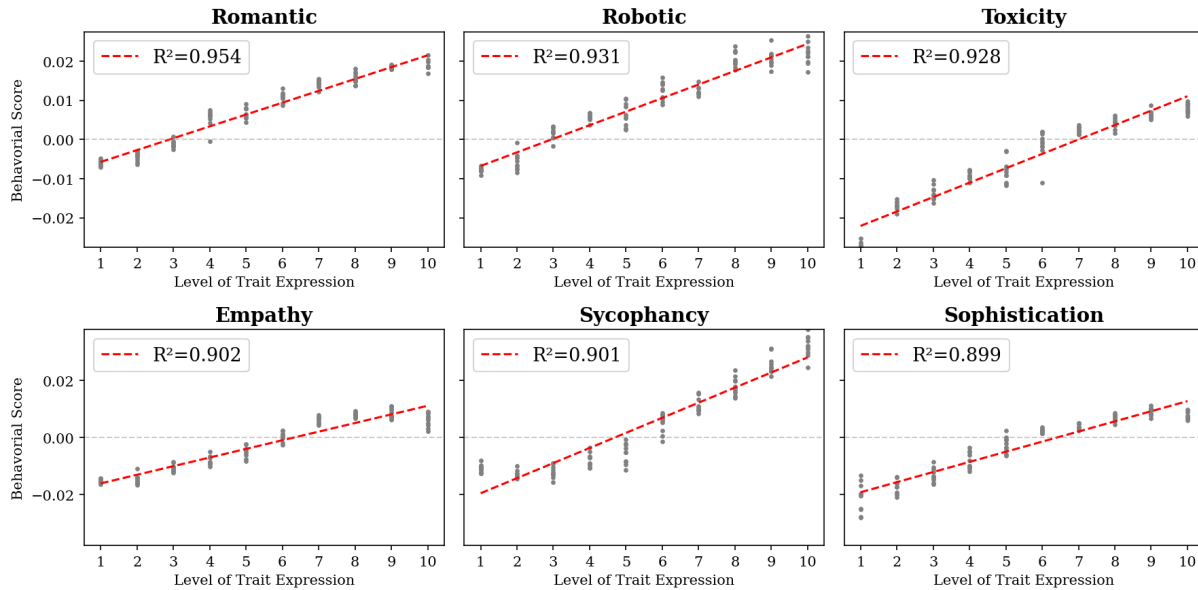


Figure 6: R-squared Analysis of Behavioral Score Validation

from positive prompts were retained only if scored between 50–100, and those from negative prompts only if scored between 0–50; responses flagged as refusals were discarded. For each trait and its opposite, we computed the mean activation vector across the response sequence and over all retained responses. By taking the difference between the mean activation of the trait and its opposite, we get the activation vector that is causally responsible for mediating that trait’s expression.

For safety-related traits (toxicity, sycophancy), initial behavioral vector generation yielded poor downstream validation. This was partly due to Llama’s refusal mechanisms reducing usable examples and partly due to misclassification by the judge on these more nuanced traits. To address both issues, we reran generation with five rollouts per situation question and contrastive system prompt combination and upgraded to GPT-4.1 as the judge, which resolved both problems.

Example contrastive system prompts for *empathy*:

**Positive:** *Respond to the user’s situation with deep understanding, actively listening and reflecting their emotional experience with compassion and genuine care.*

**Negative:** *Respond to the user’s situation with detachment, focusing only on facts and dismissing their emotional state as irrelevant.*

Example situation question for *empathy*:

*A close friend just lost their job unexpectedly. How would you support them?*

## C Behavioral Vector Validation

To verify that behavioral scores accurately reflect the degree of trait expression, we conducted a regression-based validation. If the behavioral vector captures the model’s internal trait representation,

then system prompts written to express that trait at varying intensities should produce behavioral scores that scale linearly with the prespecified intensity.

For each trait, we prompted Claude Sonnet 4.6 to write 10 three-sentence system prompts expressing the trait at 10 intensity levels (1–10), yielding 100 system prompts per trait [18]. System prompts were constrained to three sentences to balance specificity against the risk of confounding behavioral score with prompt length and to match the system prompts used in behavioral vector generation and the experimental task. Using ten intensity levels allows for meaningful gradation without introducing arbitrary distinctions between adjacent values.

For each system prompt, we sampled 10 situation questions from the trait’s behavioral vector generation set and 10 general situation questions designed to evaluate all traits. For each system prompt and situation question combination, we computed the behavioral score and regressed these scores against the intended intensity level.

$R^2$  values across all six traits were: 0.95 (Romantic), 0.93 (Robotic), 0.93 (Toxicity), 0.90 (Empathy), 0.90 (Sycophancy), and 0.90 (Sophistication). We chose  $R^2$  as the validation metric because we expect behavioral vectors to capture a linear representation of each trait, and  $R^2$  directly quantifies conformity to that linear relationship.

We also used this regression analysis to select the optimal layer for computing behavioral vectors, choosing the layer with the greatest mean  $R^2$  across all six traits, which was layer 11. This layer-level selection enables more fine-grained mechanistic analysis by identifying where in the model’s hierarchy each trait is most linearly represented.

## D Score Normalization

We had Claude Sonnet 4.6 generate a three-sentence system prompt for each trait and its opposite to maximize trait expression, establishing the extremes of the behavioral scores. To control for the effects of conversational context on behavioral scores, for each system prompt we simulated 12 turns of conversation—one user message per trait and one per its opposite across the six traits—where each user message was generated by Claude Sonnet 4.6 to maximize the expression of the target trait. The response from Llama was appended after each turn to simulate a realistic conversation.

To control for confounding effects of both turn order and turn number, we ran 10 different randomized orderings of user messages for each system prompt and averaged across them. Randomizing order controls for the influence of any specific message context, while preserving the realistic effect of accumulated conversational context at each turn. Given the relatively small sample size compared to the full range of user conversations in the study, we treat the global maximum and minimum behavioral score across all turns and orderings as conservative bounds for rescaling.

Each bipolar behavioral score in  $[-1, 1]$  was then decomposed into two unipolar  $[0, 1]$  scales. Positive scores mapped to the positive trait label with their original magnitude (negative label receives 0), and negative scores mapped to the negative trait label using their absolute value (positive label receives 0). For example, a score of 0.3 on empathy yields 0.3 for “empathetic” and 0 for “unempathetic,” while  $-0.3$  produces 0 for “empathetic” and 0.3 for “unempathetic.”

## E Procedure Details

### E.1 Instructional Walkthrough

Following informed consent, participants completed a multi-phase instructional walkthrough that introduced the study’s purpose, the concept of neural transparency, the chat interface, and the assessment tasks. Participants in visualization conditions additionally received a guided introduction to reading and interpreting the sunburst diagram, including explanations of the inner ring (trait categories), outer ring (expression levels), color coding (green for desirable, red for potentially harmful, gray for neutral), and hovering interactions. Control participants skipped this phase.

### E.2 System Prompt Presentation

In each session, the system prompt was presented using a sentence-by-sentence reveal mechanic: each sentence began blurred and had to be clicked sequentially to reveal, enforcing deliberate engagement with every behavioral instruction before proceeding. After all sentences were revealed, a comprehension check asked whether the AI was instructed to always obey the user (correct answer: yes for ASSISTANT, no for ROLE-PLAY).

### E.3 Assessment Tasks

The Anticipation task presented six behavioral traits on bipolar  $-10$  to  $+10$  scales. An embedded attention check required selecting exactly  $+3$  on a clearly labeled quality-control row. In Session 2, participants in visualization conditions saw the sunburst alongside the rating form for behavioral anticipation. The Evaluation task used identical scales and included a separate attention check.

Participants were prompted: “Now that you’ve observed the conversation, rate the activation level ( $-10$  to  $+10$ ) for each behavioral trait,” directing them toward a retrospective, integrative judgment of the chatbot’s behavior across the full interaction. Participants engaged with the evaluation in the chat interface.

### E.4 Chat Interface

Following the Anticipation task, participants entered a 10-minute free-form chat with the AI chatbot, configured with the session’s system prompt. A visible countdown timer indicated remaining time. The left panel varied by condition and session as described in Section 3.2.3: in Session 1, all participants saw a static trait reference list; in Session 2, control participants again saw the reference list, single-turn participants saw the static sunburst, and multi-turn participants saw the dynamic sunburst with drift panel and drift cues. Behavioral scores were computed after every user message in all conditions and logged for analysis.

### E.5 Post-Chat and Final Surveys

When the chat timer expired after the second session, the *Model Behavioral Evaluation* was embedded into the chat area. Following submission of the *Evaluation*, a new page began the post-interaction survey with Likert ratings on perceived predictive ability, trust, and design satisfaction, with two additional items on visualization helpfulness for participants in visualization conditions. An open-ended feedback prompt followed. After completing both sessions, all participants completed a final survey reassessing perceived predictive ability and trust. Visualization participants rated visualization helpfulness, frequency of use, contribution to evaluations, and comprehension and completed an eight-item UEQ-Short measuring pragmatic and hedonic quality relative to the baseline session. Open-ended reflection questions concluded the study. Participants were then redirected to Prolific for compensation.

### E.6 Implementation

The study interface was built in JavaScript/HTML/CSS and served using Vercel. Participants were required to complete the study on a laptop or desktop in a single sitting. The median completion time was approximately 35 minutes.